Cytoskeletal mechanics of proplatelet maturation and platelet release

Jonathan N. Thon,[1,3] Alejandro Montalvo,[1] Sunita Patel-Hett,[1,2,3] Matthew T. Devine,[1] Jennifer L. Richardson,[1] Allen Ehrlicher,[1,3] Mark K. Larson,[4] Karin Hoffmeister,[1,3] John H. Hartwig,[1,3] and Joseph E. Italiano Jr.[1,2,3]

[1]Translational Medicine Division, Brigham and Women's Hospital, Boston, MA 02115
[2]Vascular Biology Program, Department of Surgery, Children's Hospital, Boston, MA 02115
[3]Harvard Medical School, Boston, MA 02115
[4]Augustana College, Sioux Falls, SD 57197

Megakaryocytes generate platelets by remodeling their cytoplasm into long proplatelet extensions, which serve as assembly lines for platelet production. Although the mechanics of proplatelet elongation have been studied, the terminal steps of proplatelet maturation and platelet release remain poorly understood. To elucidate this process, released proplatelets were isolated, and their conversion into individual platelets was assessed. This enabled us to (a) define and quantify the different stages in platelet maturation, (b) identify a new intermediate stage in platelet production, the preplatelet, (c) delineate the cytoskeletal mechanics involved in preplatelet/proplatelet interconversion, and (d) model proplatelet fission and platelet release. Preplatelets are anucleate discoid particles 2–10 µm across that have the capacity to convert reversibly into elongated proplatelets by twisting microtubule-based forces that can be visualized in proplatelets expressing GFP–β1-tubulin. The release of platelets from the ends of proplatelets occurs at an increasing rate in time during culture, as larger proplatelets undergo successive fission, and is potentiated by shear.

Introduction

Platelet production represents the final stage of megakaryocyte development. This process, during which a giant endomitotic cell converts into 10^2–10^3 individual platelets, is highly specialized and has great clinical significance. Thrombocytopenia is a major clinical problem encountered across several conditions, including immune (idiopathic) thrombocytopenic purpura, myelodysplastic syndromes, chemotherapy-induced thrombocytopenia, aplastic anemia, human immunodeficiency virus infection, and major cardiac surgery, among others. The magnitude of the problem is not trivial. Platelet transfusions total well over 10 million units per year in the United States, and their steady increase in demand continues to challenge the U.S. blood bank community (Sullivan et al., 2007). A better understanding of the mechanisms of platelet formation will likely lead to improved therapies for thrombocytopenia. Furthermore, the ability to control in vitro megakaryocyte expansion and maturation into platelets could result in an important source of platelets for transfusion.

The proplatelet model of platelet formation recognizes that differentiated megakaryocytes extend long, branching processes, designated proplatelets, which are comprised of platelet-sized swellings in tandem arrays that are connected by thin cytoplasmic bridges. Proplatelets have been identified both in vitro and in vivo (Leven, 1987; Leven and Yee, 1987; Tablin et al., 1990), and proplatelet-producing megakaryocytes yield platelets that are structurally and functionally similar to blood platelets (Behnke, 1969; Becker and De Bruyn, 1976; Radley and Scurfield, 1980; Tavassoli and Aoki, 1981; Choi et al., 1995; Italiano et al., 1999). Mice lacking distinct hematopoietic transcription factors have severe thrombocytopenia and fail to produce proplatelets in culture, underscoring the correlation to platelet biogenesis in vivo (Shivdasani et al., 1995; Shivdasani and Orkin, 1996; Lecine et al., 1998; Shivdasani, 2001). Because of the

Correspondence to Joseph E. Italiano Jr.: jitaliano@rics.bwh.harvard.edu

Abbreviations used in this paper: ANOVA, analysis of variance; CCD, charge-coupled device; CMFDA, 5-chloromethylfluorescein diacetate; DIC, differential interference contrast; GPIX, glycoprotein IX; HSD, honestly significant difference; MVB, multivesicular body; PP, proplatelet/preplatelet; PRP, platelet-rich plasma.

© 2010 Thon et al. This article is distributed under the terms of an Attribution–Noncommercial–Share Alike–No Mirror Sites license for the first six months after the publication date (see http://www.rupress.org/terms). After six months it is available under a Creative Commons License (Attribution–Noncommercial–Share Alike 3.0 Unported license, as described at http://creativecommons.org/licenses/by-nc-sa/3.0/).

The Rockefeller University Press $30.00
J. Cell Biol. Vol. 191 No. 4 861–874
www.jcb.org/cgi/doi/10.1083/jcb.201006102

dramatic morphological changes that occur during proplatelet production, the cytoskeletal mechanics that drive these transformations have been the focus of many studies. Nevertheless, the terminal stages of proplatelet maturation and platelet release remain poorly understood. This is due in part to significant limitations in the field, such as the asynchronous maturation of hematopoietic stem cells in culture and our inability to synchronize proplatelet production. Megakaryocyte cultures always contain a complex mix of hematopoietic stem cells, immature megakaryocytes, proplatelet-producing megakaryocytes, released proplatelets (which can range dramatically in size and shape), and platelets (Behnke and Forer, 1998; Italiano et al., 2007). As there are currently no methods available to isolate the multiple intermediate stages in platelet release, most studies to date have focused on the qualitative aspects of megakaryocyte maturation.

Physiological evidence of proplatelet production has been supported by multiple images of proplatelets extending into the sinusoidal blood vessels of the bone marrow (Behnke, 1969; Becker and De Bruyn, 1976; Kessel and Kardon, 1979). Nevertheless, these represent only static snapshots of megakaryocyte maturation in situ and have yielded competing mechanistic models of platelet release. Junt et al. (2007) recently used live imaging with multiphoton intravital microscopy to visualize platelet production in vivo. Although they demonstrate that bone marrow megakaryocytes will extend proplatelets and release fragments into the vasculature, the observations they present raise questions of their own. For example, most of the shed megakaryocyte fragments appear to greatly exceed platelet dimensions, suggesting that proplatelet morphogenesis continues in peripheral blood. Because blood is moving, individual platelet release may be assisted by intravascular shear forces as proplatelets enter and become trapped in capillaries. The largest capillary bed is in lung, and it has been reported that proplatelet counts are higher in prepulmonary vessels compared with postpulmonary vessels (Handagama et al., 1987), whereas platelet counts are higher in the latter. However, evidence of a dependence of proplatelet fragmentation into platelets on hydrodynamic forces is missing.

In vivo observations that validate the proplatelet model and provide clues into the final steps of platelet production also raise several questions: how do proplatelets mature into individual platelets, is there an intermediate structure as proplatelets convert into platelets, what cytoskeletal forces are involved, and does vascular shear regulate individual platelet release? This study defines the multiple intermediate stages in proplatelet maturation and begins to identify relevant mechanistic interactions leading to platelet release from proplatelets.

Results

Characterization of the morphological stages as proplatelets mature into platelets

To study distinct stages in platelet production in vitro, released proplatelets were isolated by a novel centrifugation and gradient sedimentation protocol (Fig. S1). Enriched proplatelet populations were prepared from megakaryocyte cultures at times of maximal proplatelet elaboration and characterized for the presence/absence of a nucleus, morphology, and size (Fig. 1 A) after double staining for nuclei and tubulin (microtubules). This enabled us to define and quantify different stages in platelet maturation and identify a new intermediate stage in platelet production, the preplatelet. Preplatelets are anucleate discoid particles considerably larger (2–10 µm) than platelets that have the capacity to reversibly convert into proplatelets (anucleate beaded strings with platelet-sized tear drops at each end) during cell culture. Fig. 1 B shows the distribution of cellular elements in a fresh preparation after the removal of most megakaryocytes; a few megakaryocytes (<1% of the total number of objects) contaminate the cultures, although immature intermediates (proplatelets and preplatelets) and platelets make up the bulk of the culture. Proplatelets were subdivided into two groups by their perimeter, large (>50 µm) or small (30–50 µm), with large proplatelets initially dominant. Preplatelets and platelets were distinguished by their diameters (>2 µm or ≤2 µm, respectively). Large preplatelets were subdivided into four groups based on their diameters (8–10, 6–8, 4–6, or 2–4 µm). These were quantified and normalized to total proplatelet/preplatelet (PP) counts to account for variability in density between different preparations. Proplatelets and preplatelets were equally distributed and comprised ∼62% of the total number of objects. The majority (69%) of preplatelets have small (2–4 µm) diameters, approaching the size of mature platelets. The rest of the preplatelets were distributed as follows, based on their diameters: 4–6 (25%), 6–8 (4%), and 8–10 µm (2%). EM revealed that preplatelets are discoid because they have a cortical microtubule band and contain materials destined for platelets, such as secretory granules, invaginated membranes, and mitochondria (Fig. 1 C). This is expected if larger PPLT progenitors generate multiple smaller intermediates, which themselves go on to release two or more individual platelets. From estimates of cytoplasmic volume based on EM images, the largest preplatelets carry sufficient material to generate 6–20 mature platelets. 37% of the elements in the enriched proplatelet culture were platelet sized and appeared identical to platelets from mouse blood after tubulin staining. These were presumably left over after the final centrifugation step and represent platelets generated at an earlier point in culture.

Proplatelets/preplatelets can mature into platelets in vivo

Although proplatelet release (Junt et al., 2007) suggests fragmentation into platelets in blood, this supposition has not ever been observed or formally demonstrated. To establish that platelet release/maturation can occur within the blood vasculature, freshly enriched preplatelet/proplatelet isolates were 5-chloromethylfluorescein diacetate (CMFDA) labeled (Fig. 2, A and C [top]) and transfused into mice. CMFDA-labeled blood platelets were used as a control in parallel transfusions. Fig. 2 C (bottom) shows combined immunofluorescence and differential interference contrast (DIC) photographs of the platelet fraction from the blood of these mice 2 h after the proplatelet or platelet transfusion. CMFDA-labeled platelets recovered in the blood of recipient mice are identified, and when proplatelets

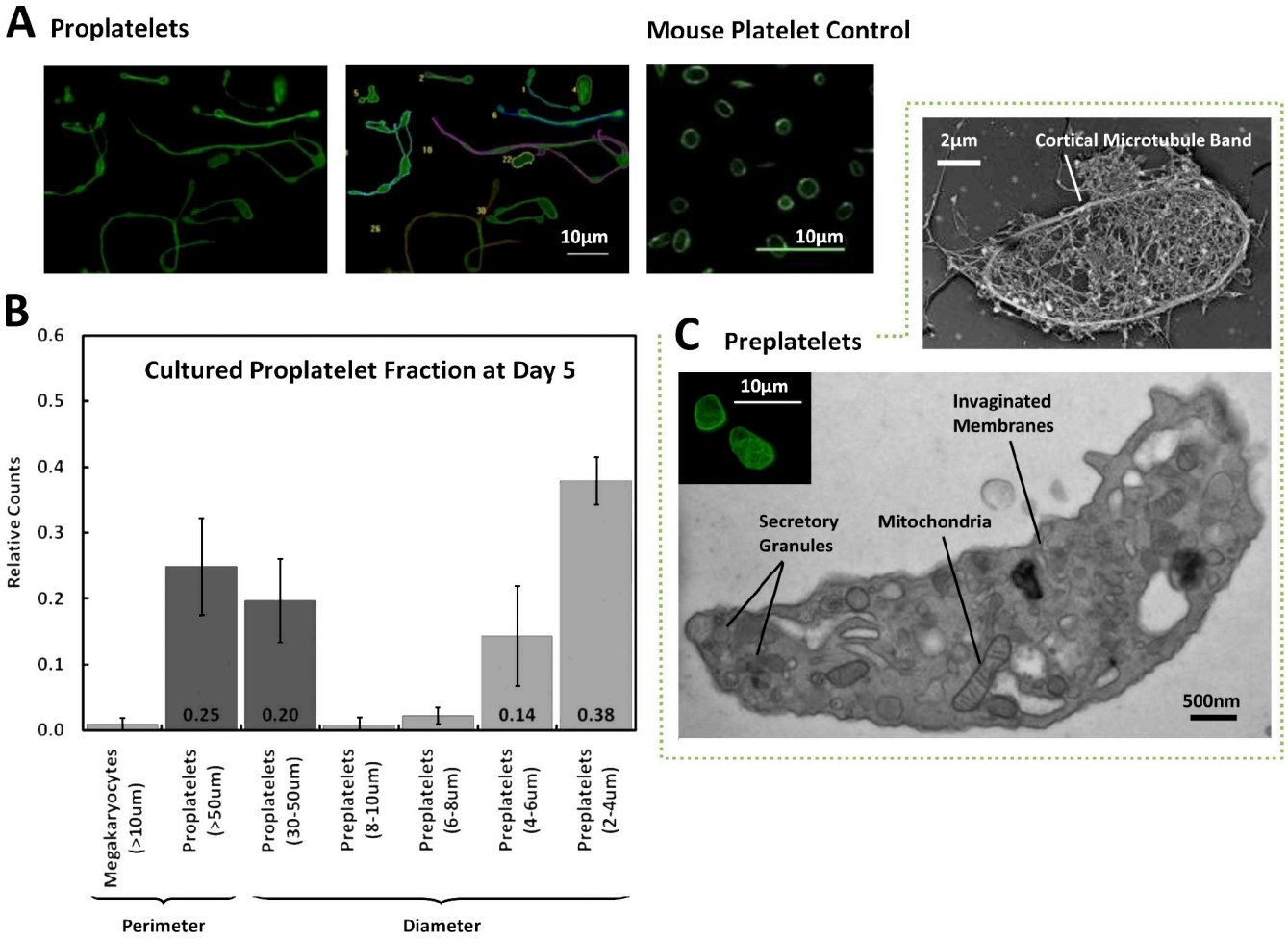

Figure 1. **Identification and quantification of intermediates in platelet release by immunofluorescence microscopy.** The released proplatelet-enriched fraction and washed mouse platelets (control) were probed with a rabbit polyclonal antibody against detyrosinated tubulin and analyzed by immunofluorescence microscopy for different-sized objects. Intermediates in platelet release were categorized based on perimeter (proplatelets) or diameter (megakaryocytes, preplatelets, and platelets). (A) Representative pictures of a day 5 proplatelet-enriched culture before (left) and after (middle) thresholding of anti-tubulin–labeled intermediates using MetaMorph software and washed mouse platelets (0.5–2-µm diameter; right). (B) Relative distribution of intermediates at day 5 of culture after proplatelet enrichment. (C) Representative pictures of the tubulin cytoskeleton of mouse preplatelets (2–10-µm diameter; immunofluorescence microscopy; inset), their ultrastructure (thin-section EM; bottom), and cytoskeleton (rapid-freeze EM; top).

were infused, this demonstrates platelet formation in blood. To quantitate platelet release, CMFDA-labeled proplatelets were transfused into mice, and blood samples were collected at regular intervals over a period of 72 h, commencing <2 min after infusing the proplatelets. Platelet-rich plasma (PRP) was isolated from the obtained blood samples, and the PPs and platelet-sized fractions were dissected and analyzed by flow cytometry (Fig. 2, A and B; Baker et al., 1997; Hoffmeister et al., 2003a). The percentage of labeled platelets in the blood at the first time point (~2 min) after transfusion is used as 100%. When platelets are transfused, they rapidly distribute in the blood volume and their blood concentration decreases thereafter, depending on the circulatory lifespan of the platelets (half-life, ~1.5–2 d in mice). However, when the immature PPs were transfused, there was a time-dependent increase in the number of labeled platelet-sized particles in blood as the infused proplatelets convert into platelets. Platelet release from the infused proplatelets was maximal by 12 h, after which the labeled platelet numbers begin to decrease, as expected again from the platelet lifetimes in blood. Further analysis of the flow cytometry data reveals that the PP fraction is rapidly sequestered after its infusion into mice; e.g., PPs are not found in blood in the initial 1:1 ratio to platelets present in the samples. In addition, the increase in CMFDA-labeled platelet counts is faster in vivo than occurs for platelets in culture (Fig. S2, B, C, and E), suggesting that blood flow–induced shear stress and/or receptor-mediated signaling may accelerate platelet release.

Platelet release in culture

The variety of different-sized preplatelets in the proplatelet culture suggested to us that we were observing an ongoing maturation program and that by studying it in vitro, we could establish precursor–product relationships between the various intermediates. We first qualified proplatelet fission (Fig. 3 A) and platelet release (Fig. 3 B) in the proplatelet cultures by video-enhanced DIC microscopy. During this process, the connection between swellings on proplatelets thins dramatically and then snaps, at which point the fragmented ends retract toward their daughter cells.

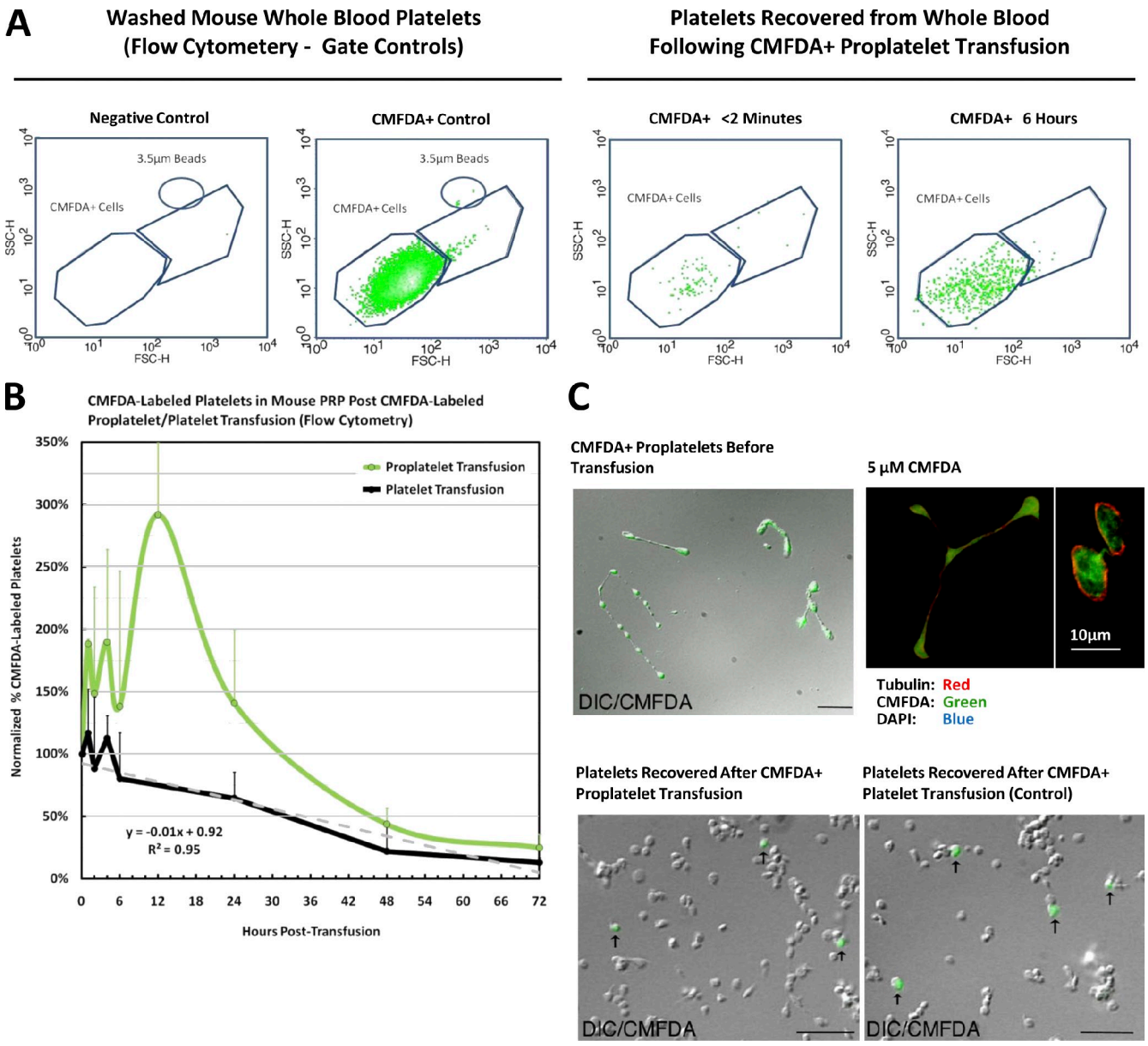

Figure 2. **Released proplatelets mature into multiple individual platelets in vivo.** (A) Washed mouse whole blood platelets were run directly on the flow cytometer (negative control) or labeled with 5 µM CMFDA before analysis (CMFDA+ control). The CMFDA+ mouse whole blood platelet population was used to establish forward/side scatter and fluorescent intensity parameters used to identify newly released platelets. Released proplatelets from mouse fetal liver cell culture were labeled with 5 µM CMFDA and transfused into live mice. PRP was collected immediately after transfusion (CMFDA+ <2 min) and 6 h after transfusion (CMFDA+ 6 h), and analyzed by flow cytometry. CMFDA+ platelets were identified using the aforementioned gates. CMFDA-labeled platelet counts were comparable at <2 min after transfusion in CMFDA-labeled platelet and cultured proplatelet transfused mice (≥1% platelet recovery and ≥0.1% of circulating platelets). (B) CMFDA-labeled proplatelets were transfused into mice, and whole blood samples were collected via retro-orbital bleeding at regular intervals over a period of 72 h, commencing with a <2-min time point. PRP was isolated, and platelets were analyzed by flow cytometry and immunofluorescence microscopy. (C) Representative pictures of CMFDA-labeled proplatelets before transfusion and mouse PRP after CMFDA-labeled proplatelet and platelet transfusions. Fluorescence and DIC images were overlaid and merged. Arrows indicate CMFDA-labeled platelets recovered from recipient mice 2 h after transfusion, demonstrating maturation of released proplatelets into multiple individual platelets within the circulatory system. Released PPs were also stained for tubulin (red) and DAPI (blue) to confirm CMFDA labeling of proplatelets before transfusion. CMFDA fluoresces at 458 nm and is shown in green. Immunofluorescence images are exhibited as a montage of representative cells from the same sample slide. Error bars indicate mean ± standard deviation.

In certain thin-section electron micrographs, a small constriction, resembling a cleavage furrow (similar to that described previously; Schwertz et al., 2010), is found in the proplatelet shaft (Fig. 3 C).

Platelet production was quantified using the combination of flow cytometric analysis and immunofluorescence microscopy to identify mature platelet-sized particles (2 µm in diameter) expressing the platelet-specific glycoprotein IX (GPIX) on their surface and/or having a cortical microtubule coil in the cultures. Mouse blood platelets served as size controls for these experiments (Fig. S2 A). Morphometry and flow cytometry showed that the number of large PP progenitors decreased

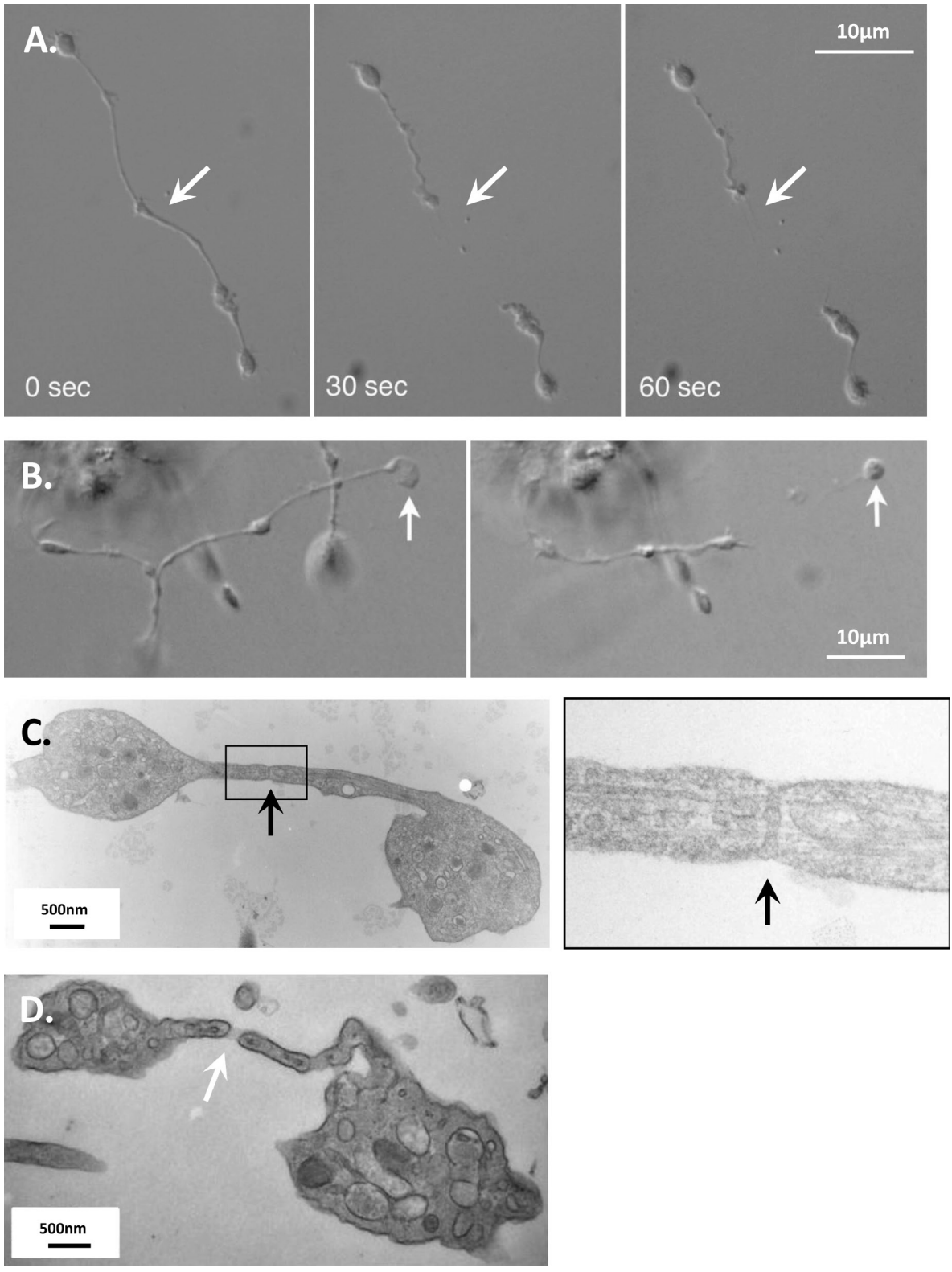

Figure 3. **Direct visualization of proplatelet/platelet release in culture.** (A and B) Isolated proplatelets were diluted with a semisolid culture medium and maintained in custom BSA-coated chambers at 37°C. They were examined on an inverted microscope, and frames were captured at 30-s intervals. (A) The separation of proplatelet cytoplasm and associated release of a shorter proplatelet fragment. The arrows highlight the site of proplatelet division. (B) The release of an individual platelet (arrows) from the end of a larger released proplatelet. (C and D) Thin-section electron micrographs showing the ultrastructure of a barbell-shaped proplatelet in the process of platelet release. Black arrows highlight the formation of a constricted region resembling a cleavage furrow along the long shaft of a cultured proplatelet. (C, inset) A higher magnification view of the boxed area is shown. (D) A similarly shaped barbell proplatelet immediately after cleavage. The arrow highlights the site of proplatelet division.

with culture time as platelet counts increased about fourfold (Fig. S2, B and C).

Fig. S4 B illustrates the distribution of PP/platelet progeny (1–137 μm^2) and proplatelet progenitors (138–227 μm^2) binned by object area and normalized to day 5 counts after 2, 24, 48, and 72 h in a representative culture and confirms an inverse relationship between smaller and larger object counts over time. Fig. S4 C illustrates the distribution of proplatelet/platelet progeny (1–137 μm^2) after 2, 24, 48, and 72 h in culture and demonstrates proplatelet fission and platelet release at an increasing rate in time.

Reversible conversions between preplatelets and proplatelets

Because the intermediates in platelet production distribute evenly between elongated proplatelets and discoid preplatelet in the cultures, we hypothesized that the two forms were interrelated. To test this hypothesis, we asked whether manipulation of microtubules within these structures could convert barbell proplatelets to preplatelets and vice versa. Released proplatelet cultures were incubated at either 37°C (normal control), 4°C for 1 h to depolymerize microtubules, or at 4°C for 1 h and then 37°C for 1 h to depolymerize and repolymerize microtubules. Fig. 4 displays log difference in total proplatelet, preplatelet, and platelet counts at 4°C (Fig. 4 A) and 4–37°C (Fig. 4 B) relative to 37°C control. Counts of proplatelets and preplatelets were performed as previously described, and all values were normalized to 37°C controls. Data were subject to one-way analysis of variance (ANOVA) for three independent samples and Tukey honestly significant difference (HSD) analysis ($P < 0.01$ and $P < 0.05$). Depolymerization of tubulin at 4°C significantly shifted the proplatelet population to preplatelet forms (Fig. 4 A). The proplatelet population returned to normal when the samples were returned to 37°C (Fig. 4 B), indicating that the proplatelet structure is a result of tubulin polymerization and microtubule organization about its midbody.

This observation was confirmed using a second method of microtubule manipulation, wherein released proplatelet cultures were incubated at 37°C in the presence of a microtubule-stabilizing agent (5 µM taxol) or a tubulin-depolymerizing agent (5 µM nocodazole) for 1 h. Counts of proplatelets and preplatelets were performed, and all values were normalized to no-drug controls. Fig. 4 C illustrates a shift in the distribution of the released proplatelet culture population toward smaller proplatelet or preplatelet forms in the presence of taxol or nocodazole, respectively. Representative pictures of proplatelet-enriched cultures after taxol or nocodazole incubations appear in Fig. 4 D. These results suggest that the microtubule cytoskeleton of intermediates in platelet production undergo a dramatic reorganization during their interconversion between preplatelet and barbell proplatelet forms. Moreover, the pharmacological regimen used suggests that the reorganization of microtubules plays an essential role in this morphogenesis.

Mechanisms of proplatelet maturation and platelet release

Having established a precursor–product relationship between proplatelets–preplatelets and proplatelets–platelets, we investigated the underlying mechanisms. Three types of behaviors were studied in detail: (1) the proplatelet–preplatelet interconversions, (2) fission of small proplatelets into platelets, and (3) shear-facilitated proplatelet fission and platelet release. Proplatelets and preplatelets are distinguished from their elongated or discoid shapes, respectively. However, both have prominent cortical microtubule bundles. In preplatelets, these bundles rim the cytoplasmic surface of the membrane on the disc face. In proplatelets, the bundles also rim the cell membranes of the bulbous particles, but they collapse together and interact along the shafts. The exponential accumulation of smaller PPs and platelets in our culture system over time implies a model in which larger proplatelet progenitors undergo continuous fission, producing an increasing number of sequential platelet release sites.

Direct visualization of microtubule dynamics during the conversion of preplatelets to barbell proplatelets

To visualize the microtubule cytoskeleton directly during preplatelet to barbell proplatelet conversion and to confirm this relationship between the two intermediate structures, cultured megakaryocytes were retrovirally directed to express GFP–β1-tubulin. Released proplatelet fractions were isolated, and GFP–β1-tubulin–labeled preplatelets were monitored by fluorescence time-lapse microscopy. Fig. 5 A depicts a representative preplatelet of ∼7 µm in diameter over a period of 4 min. In this time, the oval marginal band was observed to twist about its center several times in a clockwise fashion to ultimately yield a barbell-shaped proplatelet with two well-defined platelet-sized (2-µm diameter) microtubule loops at each end. This was confirmed by thin-section EM (Fig. 5 B). Fig. 5 C shows the microtubule cytoskeleton twisting about the preplatelet center to yield a "figure 8" structure comparable with Fig. 5 A (1 min) and suggests an intermediate stage in preplatelet to proplatelet interconversion.

To establish whether microtubules continue to polymerize throughout released proplatelets once defined microtubule loops have formed, mouse megakaryocyte cultures were retrovirally directed to express EB3-GFP. EB3-GFP localizes only at polymerizing microtubule plus ends in a characteristic comet staining pattern with a bright front and dim tail (Fig. S3). Fig. S3 shows the first frame from Video 4, a time-lapse video of a cultured proplatelet expressing EB3-GFP. Multiple comets are observed moving bidirectionally in the cytoplasmic bridge and within the microtubule coil at the ends of the proplatelet, confirming continued dynamic assembly and reorganization of microtubule coils at a late stage of proplatelet development. Comet movement rates are estimated to be ∼8.9–12.3 µm/min.

Multivesicular bodies (MVBs) are present and granules continue to sort in released proplatelet/preplatelet intermediates

The biogenesis and distribution of platelet-specific granules into nascent platelets are essential to platelet production. In megakaryocytes, MVBs represent a developmental stage in α-granule and dense-granule maturation (Heijnen et al., 1998; Youssefian and Cramer, 2000). Indeed, differences in intragranular protein distribution of MVBs, α-granules, and dense granules have been

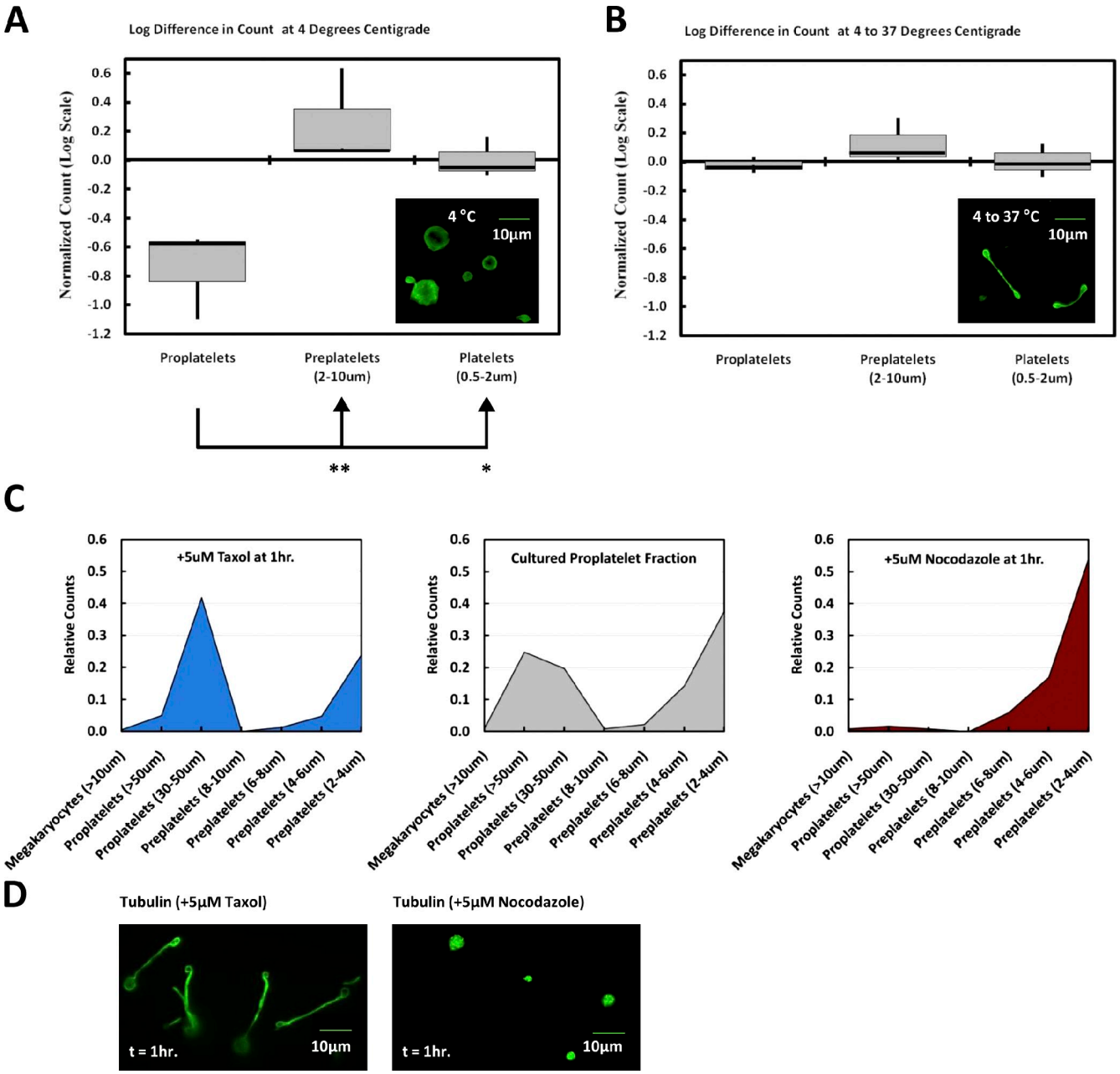

Figure 4. **Preplatelets reversibly convert into proplatelets using microtubule-based forces.** (A and B) Proplatelet-enriched fractions were probed with a rabbit polyclonal antibody against detyrosinated tubulin and analyzed by immunofluorescence microscopy for different-sized objects. Samples were incubated at 37°C (normal control), 4°C for 1 h, or 4°C for 1 h and returned to 37°C for 1 h. All values were normalized to the 37°C controls. (A) Depolymerization of tubulin at 4°C shifted the proplatelet population into preplatelet forms. *, $P < 0.05$; **, $P < 0.01$. Arrows indicate values compared and significance level of difference. (B) The proplatelet population returned to normal upon repolymerization of tubulin at 37°C. Data were subject to one-way ANOVA for three independent samples and Tukey HSD analysis. (C) Released proplatelet/platelet fraction from second gradient sedimentation probed with a rabbit polyclonal antibody against detyrosinated tubulin and analyzed by immunofluorescence microscopy for different-sized objects. Distribution of proplatelet and preplatelet forms after 1 h in culture with 5 µM taxol (promotes microtubule polymerization; left), a vector control (middle), or 5 µM nocodazole (promotes microtubule depolymerization; right). Microtubule stabilization and depolymerization shifted the population toward proplatelet and preplatelet forms, respectively. (D) Representative pictures of cultured intermediates after taxol (proplatelet) or nocodazole (preplatelet) incubations.

reported previously (van Nispen Tot Pannerden et al., 2010) and may reflect effective sorting and/or retention mechanisms in their formation. Nevertheless, it is unclear whether granule biogenesis occurs in preplatelets or released proplatelets. To address this question, we looked for MVBs in released proplatelets and preplatelets. Thin-section EM revealed the presence of MVBs in structural intermediates of platelet production (Figs. 6 A and S5), which may suggest ongoing granule biogenesis in these cells.

Transport of organelles along proplatelets involves movement along microtubules and translocation of linked microtubules relative to one another (Richardson et al., 2005). Barbell proplatelets have a dynamic microtubule cytoskeleton that continues to assemble and reorganize during late-stage platelet development.

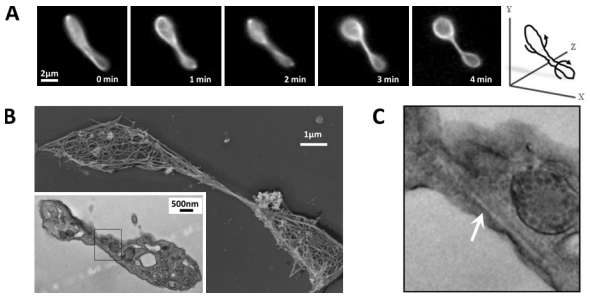

Figure 5. **Microtubule dynamics during the conversion of preplatelets to barbell-proplatelets.** (A) Fluorescent time-lapse microscopy of a released preplatelet isolated from megakaryocytes retrovirally directed to express GFP–β1-tubulin. The oval preplatelet microtubule marginal band is observed to twist about its center several times in a clockwise fashion over the course of 4 min to yield a barbell-shaped proplatelet with well-defined microtubule loops at each end. (B) Rapid-freeze and thin-section electron micrographs showing the cytoskeleton and ultrastructure of microtubules in proplatelets. (C) High magnification electron micrograph of the boxed region in B shows microtubules twisting about the proplatelet center to yield a "figure 8" structure.

This raised the question of whether organelles continue to sort between platelet-sized swellings in these structural intermediates. To resolve the localization and distribution of secretory granules in the preplatelet and released proplatelet during interconversion, cultures were either labeled with a fluorescent human fibrinogen conjugate (taken up and stored in α-granules) or probed for serotonin (present in dense granules) and analyzed by immunofluorescence microscopy. The distribution and dynamics of the labeled α-granules were followed using time-lapse fluorescence microscopy and demonstrate ongoing, bidirectional α-granule movement during preplatelet–proplatelet conversion (Fig. 6 B). Video 1 also demonstrates the elongation that precedes the fission-like process that accompanies preplatelet to barbell proplatelet conversion. α-Granules localize to the microtubule cytoskeleton and are generally confined to the periphery of the cell. Fig. 6 C illustrates continued and bidirectional translocation of fluorescently labeled α-granules in a barbell proplatelet over a period of 36 min. Red dots highlight α-granule movement toward the top end of the proplatelet, whereas green dots highlight movement toward the bottom end. Labeled organelles moved bidirectionally along the microtubule tracks of cytoplasmic bridges and cortices of developing proplatelets at a rate of ∼0.13–0.26 µm/min, implying continued reorganization of platelet contents through late stages of the maturation process. This is also true of dense granules, which distribute within the preplatelet and along the cytoplasmic bridges and bulbous tip of released proplatelets (Fig. 6 D). Like the α-granules, these continue to translocate throughout maturation.

Shear forces accelerate proplatelet fission and platelet release in vitro

To determine whether platelet production from released PP intermediates could be accelerated by circulatory shear forces, isolated PPs were maintained in culture under static conditions or with continuous shear (∼0.5 Pa) for 2 h and analyzed by immunofluorescence microscopy and flow cytometry at 20-min intervals. Fig. 7 (A–C) shows composite images of the proplatelet culture after 0, 60, and 120 min of shear. Compared with the no shear control, platelet numbers increased, whereas the number of proplatelets decreased over time (Fig. 7 D). Platelet and PP progeny (1–137 µm^2; Fig. 7 E) and proplatelet progenitors (138–227 µm^2; Fig. 7 F) were binned by size (area), and their relative counts over time were spread across multiple bins to resolve the mechanism of platelet release. The data describe an inverse relationship between smaller and larger object counts that suggests dynamic proplatelet fission and continuous platelet release under shear with time. Flow cytometric analysis of cultured samples agree with immunofluorescence microscopy data and reveal a significant decrease in the number of large proplatelets and PP intermediates (small ProPLTs) after 2 h relative to no shear control (Fig. 7, G and H). Fig. 8 summarizes the model of platelet production from proplatelets supported by these experiments.

Discussion

The presence of proplatelets in blood implies that they fragment into individual platelets. To evaluate the mechanisms by which released proplatelets mature platelets and to identify intermediate stages in this process, we developed a novel centrifugation and gradient sedimentation protocol to separate megakaryocytes and residual megakaryocyte cell bodies from released proplatelets. This enabled us to define and quantify different stages in proplatelet maturation and platelet release, relate these temporal changes to cytoskeletal rearrangements, and begin to describe some of the mechanistic events that ultimately lead to platelet release.

To define the relative distribution of these different-sized objects over time and to place the appearance and accumulation of individual platelets in a temporal context, intermediates in platelet release were categorized by their morphologies and size. This allowed changes in distribution to be tracked over a period of 5 d in culture. In addition to mature discoid platelets and elongated proplatelets, we identified a large, intermediate discoid stage in platelet production, which we have named the "preplatelet." Preplatelets are large anucleate discs, 2–10 µm in diameter, that have a thick cortical microtubule coil and retain the capacity to reversibly convert into barbell-shaped proplatelets. Continued bidirectional polymerization of microtubules at each end of the barbell proplatelet forms two well-defined platelet-sized (2-µm diameter) microtubule loops at each end. These become two individual platelets after a fission event. Interestingly, interconversion between preplatelet and proplatelet forms occurs only at preplatelet diameters 2–10 µm across. Thus, preplatelets represent an intermediate stage in platelet production that may be responsible for regulating platelet size. Although larger microtubule coils may undergo twisting to accommodate continued microtubule polymerization/elongation within a constrained volume, forming barbell proplatelets, smaller, more constricted microtubule coils are unable to do so. As megakaryocyte fragments divide (thus becoming smaller), this results in a size limit beyond which new platelets are no longer capable of fission and may therefore provide an artificial margin from which platelets can be classified as distinct from their progenitors.

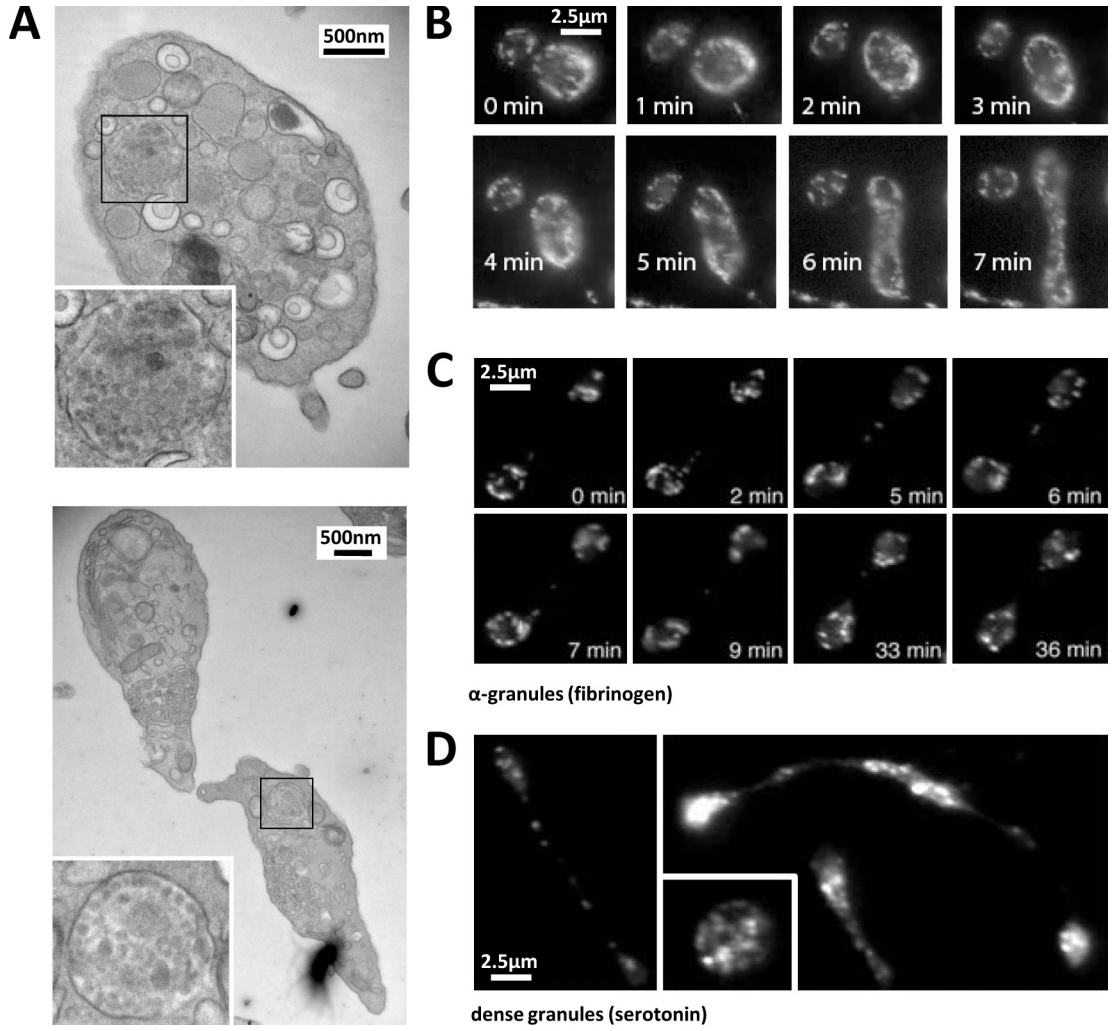

Figure 6. **Granules are synthesized, packaged, and continue to sort in released proplatelets.** (A) High magnification electron micrographs show the presence of MVBs in released preplatelets (top) and proplatelets (bottom). (B and C) Mouse preplatelet/proplatelet labeled with a fluorescent human fibrinogen conjugate, which is taken up and stored in α-granules. The distribution and dynamics of the labeled α-granules were followed using time-lapse fluorescence microscopy and demonstrate ongoing, bidirectional α-granule movement during preplatelet to proplatelet conversion. (C) Red dots highlight α-granule movement toward the top end of the proplatelet, whereas green dots highlight movement toward the bottom end. Labeled organelles moved bidirectionally along the microtubule tracks of cytoplasmic bridges and cortices of developing proplatelets at a rate of ∼0.13–0.26 µm/min, implying continued organization of platelet contents through late stages of the maturation process. The width of the field is 10 µm. (D) Released proplatelet/platelet fraction from second gradient sedimentation probed with a rabbit monoclonal antibody against serotonin. Fluorescence and DIC images were overlaid and merged. Images are exhibited as a montage of representative cells from the same sample slide. Dense granules distribute evenly within the preplatelet and along the cytoplasmic bridges and bulbous tip of released proplatelets and continue to translocate throughout maturation.

Interestingly, Schwertz et al. (2010) have recently published findings demonstrating that platelets isolated from circulating human blood may duplicate through a process that morphologically resembles preplatelet to proplatelet interconversion. Their observation that ∼5% of washed platelets extended projections with distinct cell bodies after only 6 h of culture is consistent with the relative proportion of large platelets identified in circulating blood (unpublished data). As megakaryocyte cell fragments 2–10 µm in diameter are able to interconvert between preplatelet and barbell proplatelet forms, it is tempting to speculate that our observations are related.

In vivo, released proplatelets and preplatelet-like structures significantly larger than platelets are often observed in mouse whole blood at elevated concentrations 96 h after thrombocytopenia induced by rabbit anti–mouse platelet serum injection. These subsequently decrease in size over time to that of normal platelets as the count returns to baseline (Patel-Hett et al., 2008). When CMFDA-labeled proplatelets are transfused into recipient mice, platelets rapidly release for a period of 12–24 h. In vitro, proplatelets slowly mature into multiple individual platelets over a 5-d culture period, as total proplatelet and preplatelet counts decrease about sevenfold, whereas platelet counts increase about fourfold. Thus, this intermediate stage may correlate to the young, large platelets found during recovery from acute thrombocytopenia, such as that in immune-mediated platelet destruction (Patel-Hett et al., 2008), and they may represent the submegakaryocyte fragments observed previously in PRP (Behnke and Forer, 1998).

As proplatelets are not generally seen at concentrations comparable with those of platelets in healthy human and mouse

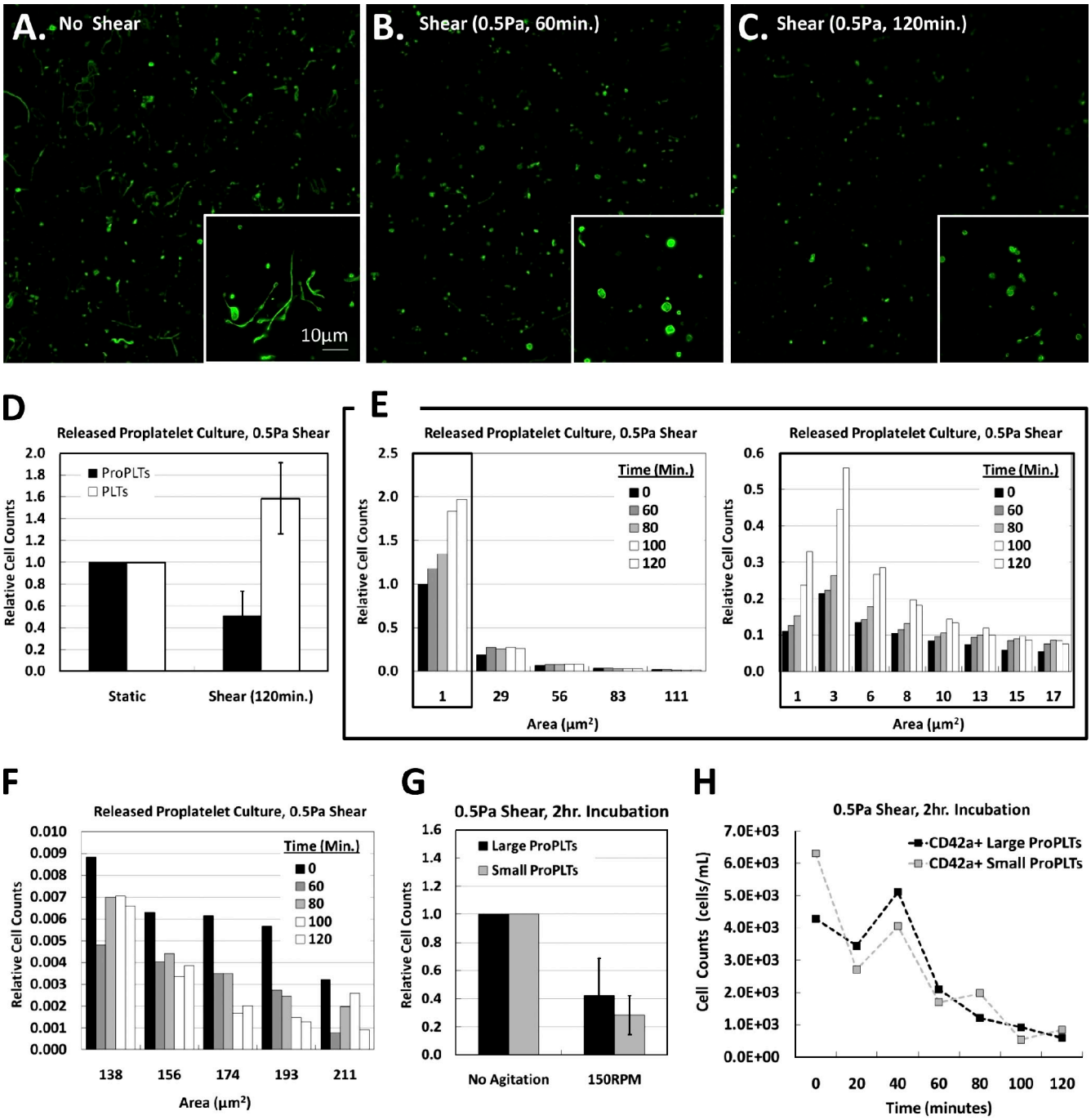

Figure 7. **Shear force promotes proplatelet fission and platelet release.** (A–H) Proplatelets released from fetal liver–derived megakaryocytes were cultured for 2 h in the presence or absence of shear (~0.5 Pa). Every 20 min, samples were removed and probed with a rabbit polyclonal antibody against β1-tubulin and analyzed by immunofluorescence microscopy for different-sized objects (A–D) or labeled with a CD42a-specifc, FITC-conjugated antibody and analyzed by flow cytometry (G and H). (A–C) Representative micrographs of the culture after 0 (A), 60 (B), and 120 (C) min of shear. (insets) High magnification views of the composite images are shown. (D) Compared with no shear controls, platelet numbers increased over time, whereas proplatelet numbers decreased (n = 4). (E and F) Representative quantification of culture intermediates under shear with time. Platelet and PP progeny (cells of area = 1–137 µm^2; E) and proplatelet progenitors (138–227 µm^2; F) were binned by size (area), and their relative counts over time were spread across multiple bins to resolve the mechanism of platelet release. The data describe an inverse relationship between smaller and larger object counts that reveal dynamic proplatelet fission and continuous platelet release under shear with time. (G) Flow cytometric analysis of cultured proplatelet intermediates under shear with time (n = 3). (H) Representative quantification of cultured proplatelet intermediates by flow cytometry. Samples support immunofluorescence microscopy data and reveal a significant decrease in the number of large proplatelets and PP intermediates (small ProPLTs) after 2 h relative to no shear control. Error bars indicate mean ± standard deviation.

whole blood smears, it stands to reason that the rate of platelet production in our culture system remains relatively low as compared with suspected platelet release rates in vivo. Modeling of this effect revealed that during cell culture, platelets are generated at an increasing rate in time, and large proplatelets undergo continuous fission to produce more ends from which platelets

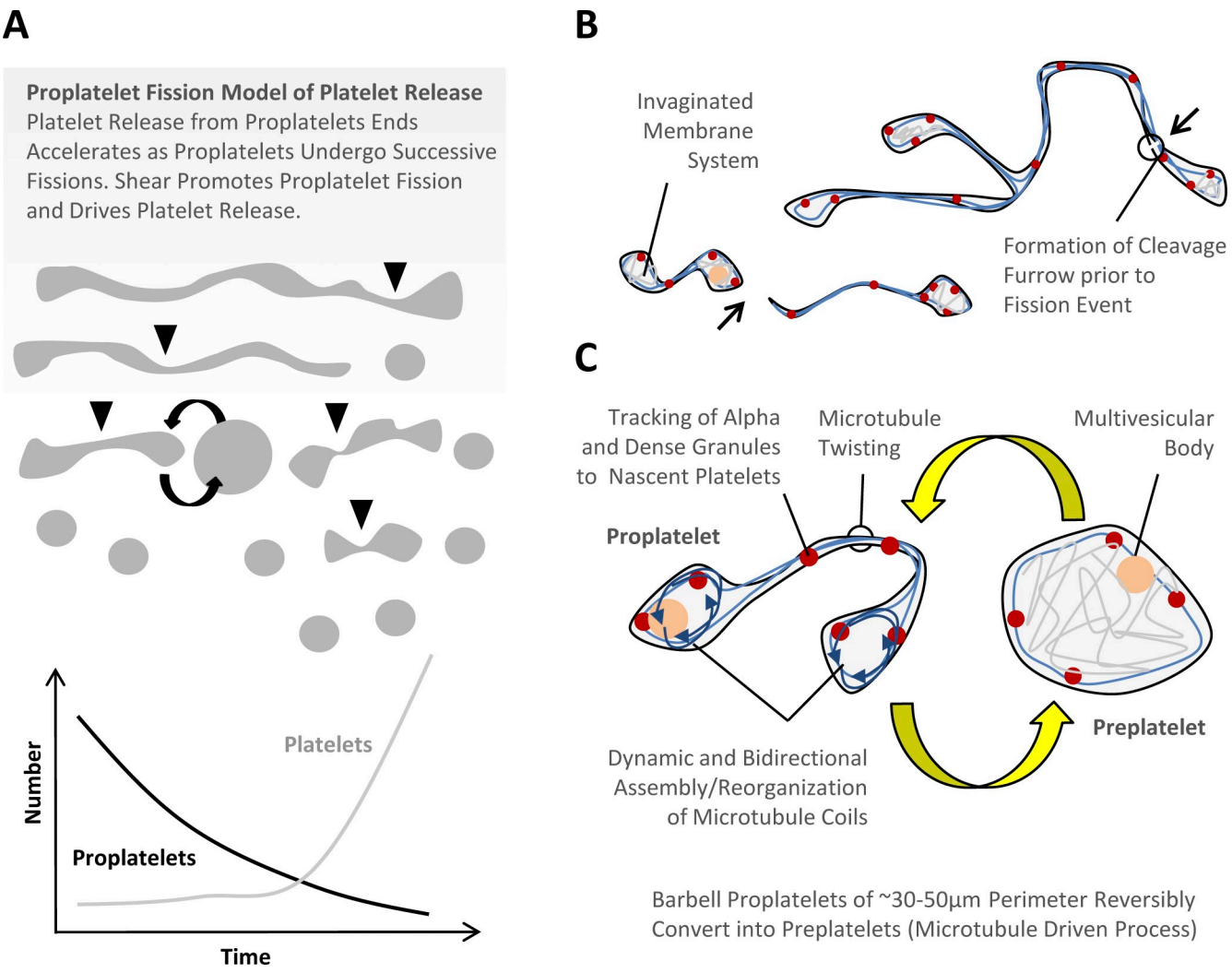

Figure 8. **Proplatelet fission model of platelet release.** Model of platelet production suggested by these experiments and previous studies (see Results). (A) Released proplatelets undergo successive rounds of fission along their midbody and at their ends. This process is mediated by the formation of a cleavage furrow at the point of division and results in platelet release from proplatelet ends at an increasing rate in time as more ends become available after each fission event. Shear promotes proplatelet fission and drives platelet release. (B) Barbell proplatelets of ~30–50-µm perimeter reversibly convert into preplatelets. This process is driven by twisting microtubule-based forces and may represent a novel mechanism of microtubule reorganization and granule redistribution after each fission event. (C) During barbell proplatelet formation, dynamic and bidirectional assembly and reorganization of microtubule coils mediate platelet cytoskeleton arrangement as α- and dense granules track to distal proplatelet tips. Platelets release from proplatelet ends after the final fission event.

are released. Indeed, relatively weak hydrodynamic forces of maximally 0.5 Pa were found to promote proplatelet fission, which is likely necessary in regulating the rate of platelet release in vivo. Flow cytometric analysis of CMFDA-labeled proplatelets transfused into live mice supports this hypothesis and suggests that blood flow–induced shear stress may contribute to platelet release in vivo by promoting proplatelet fission events. Indeed, observations that proplatelet counts are higher in prepulmonary than in postpulmonary vessels (Handagama et al., 1987), whereas platelet counts are higher in the latter, imply that shear forces act on released proplatelets in the vasculature to mediate platelet production.

The geometric decay of larger proplatelet progenitors and accumulation of smaller PPs and released platelets in our culture system over time (under both static and continuous shear conditions) implies that platelets are predominately released from proplatelet ends as proplatelets undergo continuous fission in culture. Therefore, proplatelets contain all of the programming and material required to make and release platelets, which is in accordance with the observations that bone marrow megakaryocytes extend and release large cellular processes, exceeding platelet dimensions, into blood (Junt et al., 2007).

Nevertheless, how small proplatelets, barbell-shaped proplatelets, and platelets release from larger proplatelets has never been detailed. Our video-enhanced DIC images of proplatelets in culture reveal that large proplatelets divide into shorter proplatelets and release individual platelets. As a proplatelet elongates, its long, narrow shaft will sometimes snap, dividing the structure into two pieces. This snapping and retraction is characteristic of the release of mechanical tension being applied along the process by internal cytoskeletal motors. Measured rates of proplatelet fission and platelet release show that cleavage events

occur continuously throughout the different intermediate stages of platelet production, resulting in mixed proplatelet populations of various different sizes.

Proplatelets must not only produce and replicate the specialized cytoskeleton of the mature platelet, but they must also load each platelet with a reproducible and appropriate allotment of organelles and granules essential for their hemostatic function. Our experiments demonstrate the presence of MVBs in late-stage intermediates, which represent a developmental step in α- and dense-granule maturation. One of the most surprising findings is that even at the very final stages of platelet production, when two putative platelets are connected by a cytoplasmic bridge, the granule content of the platelet is still being adjusted. It has recently been shown that platelets contain distinct subpopulations of α-granules that undergo differential release during activation (Italiano and Battinelli, 2009). Interconversion between barbell proplatelet and preplatelet forms might therefore represent a novel mechanism of granule redistribution and sorting before platelet release from proplatelet ends.

In summary, this study defines the multiple intermediate stages in proplatelet maturation and identifies several relevant mechanical interactions, which govern individual platelet release. Our understanding of the final stages of platelet production is still far from perfect, and there remain many questions that still need to be answered: (a) what factors and signal transduction pathways are involved in reorganizing the microtubule cytoskeleton to mediate PP interconversion and platelet release, (b) how do shear forces in the circulation contribute to this process, (c) is platelet production in vivo a result of sequential liberation from proplatelet ends or a product of successive fission of the released proplatelet, and (d) how do preplatelets identified in culture correlate with immature platelets observed in thrombocytopenia and large platelets observed in many macrothrombocytopenias? Nevertheless, the development of new methods to isolate and quantify the multiple intermediate stages in platelet release holds promise that these questions can now begin to be addressed.

Materials and methods

Megakaryocyte suspension cultures

Mouse fetal liver cells were recovered on embryonic day 13.5. Single-cell suspensions were prepared by successive passage through 22- and 25-G syringes and cultured for 4 d in DME (Invitrogen) supplemented with 10% fetal calf serum, 2 mmol/liter L-glutamine, 50 U/ml penicillin, and 50 µg/ml streptomycin at 37°C and 5% CO_2 in the presence of 0.1 µg/ml purified recombinant mouse c-Mpl ligand (day 0; Lecine et al., 2000). All experiments were complied with institutional guidelines approved by the Children's Hospital Animal Care and Use Committee and the Institutional Animal Care and Use Committee.

Isolation of released proplatelets/preplatelets

Fetal liver cell cultures were layered on a single-step gradient (1.5–3.0% BSA) on day 4, and megakaryocytes were allowed to sediment for 1 h as previously described (Drachman et al., 1997). The megakaryocyte pellet was resuspended in fresh media and cultured for an additional 24 h, during which proplatelet production was readily observed. Megakaryocyte cultures were layered on a second single-step gradient (1.5–3.0% BSA) on day 5. Megakaryocytes were allowed to sediment for 1 h, during which intermediate stages in platelet production were resolved within different fractions of the gradient. Proplatelet-producing megakaryocytes localized to the BSA fraction, whereas released proplatelets and individual platelets remained in the top (culture media) fraction. This top-most layer was removed and centrifuged (200 *g* for 5 min) to further separate released proplatelet (pellet) and platelet (supernatant) fractions. Samples were washed and resuspended in culture media. Cultures were kept at 37°C and 5% CO_2 throughout.

Immunofluorescence microscopy

Mouse megakaryocytes, culture intermediates, and whole blood platelets were purified and probed as previously described (Patel-Hett et al., 2008). In brief, samples were fixed in 4% formaldehyde and centrifuged onto 1 µg/ml poly-L-lysine–coated coverslips, permeabilized, and blocked (Italiano et al., 2003) before antibody labeling. Released proplatelet-enriched fractions were incubated with a rabbit polyclonal antibody against detyrosinated tubulin (SuperGlu; provided by C. Bulinski, Columbia University, New York, NY) or a rabbit monoclonal antibody against serotonin (YC5/45; Abcam) for dense-granule localization and treated with secondary goat anti–rabbit antibody conjugated to an Alexa Fluor 488 (Invitrogen). DAPI (Sigma-Aldrich) was used to label the megakaryocyte nucleus. Samples were examined with a microscope (Axiovert 200; Carl Zeiss, Inc.) equipped with a 63× NA 1.4 oil immersion objective. Images were obtained using a charge-coupled device (CCD) camera (Hamamatsu Photonics) and analyzed using the MetaMorph image analysis software (MDS Analytical Technologies). Intermediates in platelet release were categorized based on perimeter (proplatelets) or diameter (megakaryocytes, preplatelets, and platelets) using the MetaMorph software thresholding, integrated morphometry analysis, and software calipers tools. Experiments represent one standard deviation about the mean for at least seven independent cultures.

EM

Released proplatelet-enriched cultures in suspension were fixed with 1.25% paraformaldehyde, 0.03% picric acid, and 2.5% glutaraldehyde in 0.1 M cacodylate buffer, pH 7.4, for 1 h, postfixed with 1% osmium tetroxide, dehydrated through a series of alcohols, infiltrated with propylene oxide, and embedded in epoxy resin. Ultrathin sections were stained and examined with an electron microscope (G2 Spirit BioTwin; Tecnai) at an accelerating voltage of 80 kV. Images were recorded with a CCD camera (2K; Advanced Microscopy Techniques) using digital acquisition and analysis software (Advanced Microscopy Techniques). Rapid-freeze EM samples were prepared as previously described (Italiano et al., 1999). Tantalum tungsten and carbon replicas were picked up on carbon formvar–coated copper grids and examined.

Flow cytometry

Released proplatelet fractions were isolated and cultured as described in "Isolation of released proplatelets/preplatelets" and sampled daily over a period of 5 d. Platelet counts were determined by flow cytometric analysis with a primary rat IgG antibody specific for mouse GPIX (provided by B. Nieswandt, University of Wurzberg, Wurzberg, Germany) and a secondary goat anti–rat antibody conjugated to Alexa Fluor 488 (Invitrogen). Secondary antibody specificity controls were performed. Gates were set using 0.5–10-µm microspheres (Spherotech) and confirmed by DIC microscopy at 63× and 100×. Platelets were isolated from culture intermediates by their characteristic forward and side scattering as they passed through the flow cytometer, and their total fluorescence intensity was calculated after subtraction of the secondary antibody specificity control. Platelet counts were based on GPIX-positive objects 0.5–2.0 µm in size and normalized to proplatelet (GPIX positive, 3.3–10-µm particle) counts at 0 d after proplatelet enrichment. Analysis of platelet counts were performed for at least 15 different cultures. Data were subject to one-way ANOVA for four independent samples and Tukey HSD analysis. Experiments represent one standard deviation about the mean for at least three independent samples.

Released proplatelet transfusion

For proplatelet transfusion and platelet production/survival experiments, cultured released proplatelets and wild-type whole blood platelets were labeled with 5 µM CMFDA (Invitrogen) for 45 min at 37°C (Hoffmeister et al., 2003a,b; Josefsson et al., 2005) Unincorporated dye was removed by centrifugation, and (cultured) released proplatelets or (whole blood) platelets were resuspended in 300 µl of culture media or platelet buffer, respectively. CMFDA-labeled released proplatelets or control platelets were injected into syngeneic CD61 mice via retro-orbital vein. For recovery and survival determination, blood samples were collected immediately (<2 min) and 1, 2, 4, 6, 24, 48, and 72 h after transfusion into 0.2 vol Aster-Jandl anticoagulant. Whole blood PRP analysis using flow cytometry was performed, and the percentage of CMFDA-positive platelets was determined (Baker et al., 1997; Hoffmeister et al., 2003a). A total of 200,000 events were collected in each sample. CMFDA-positive platelet counts were normalized to the <2-min

time point (100%), and analyses of platelet counts were performed for at least three different transfusion events. Recoveries from CMFDA-labeled platelet and proplatelet transfusions were ≥1%, and the percentage of circulating labeled platelets, determined at <2 min, was ≥0.1%.

DIC live cell microscopy

Isolated proplatelets were diluted in a semisolid medium (60% Leibowitz L-15 medium and 40% DME with 10% fetal bovine serum, 50 U/ml penicillin, and 50 µg/ml streptomycin) in chambers formed by mounting a glass coverslip coated with 3% BSA onto a 10-mm petri dish with a 1-cm hole. Preparations were maintained at 37°C and examined on an inverted microscope (Axiovert 200) equipped with a 63× NA 1.4 objective, an XL-3 incubation chamber, and a 100-W mercury lamp (Carl Zeiss, Inc.). Images were obtained using a CCD camera (Hamamatsu Photonics), and frames were captured at 30-s intervals. Videos 1–4 were generated using the MetaMorph image analysis program.

Stabilization/depolymerization of released proplatelet microtubule cytoskeletons

Released proplatelet cultures were incubated at (a) 37°C (normal control) or 4°C for 1 h and again at 37°C for 1 h or (b) in the presence of 5 µM taxol or 5 µM nocodazole for 1 h at 37°C. Samples were centrifuged onto poly-L-lysine–coated glass coverslips and probed with a rabbit polyclonal antibody against detyrosinated tubulin then analyzed by immunofluorescence microscopy for different-sized objects. All values were normalized to the 37°C (normal) controls, and experiments were performed in triplicate. Box and whisker plots illustrate sample minimum, lower quartile, median, upper quartile, and sample maximum for samples cultured at 4°C. Data were subject to one-way ANOVA for three independent samples and HSD analysis.

Expression of GFP–β1-tubulin and EB3-GFP constructs

GFP–β1-tubulin was cloned into pWZL plasmids containing the sequence for enhanced GFP using previously described methods (Schulze et al., 2004). The released proplatelet fraction was isolated from megakaryocytes that were retrovirally directed to express GFP–β1-tubulin and analyzed by fluorescence time-lapse microscopy. Semliki Forest virus–mediated gene delivery was used to express EB3-GFP in mouse megakaryocytes (Patel-Hett et al., 2008). Cultured megakaryocytes were infected by the addition of 1 µl Semliki Forest virus infectious replicons to 400 µl day 2.5 cultures. EB3-GFP movements were visualized by fluorescence microscopy 8–48 h after infection.

Live cell imaging of GFP–β1-tubulin, EB3-GFP, and α-granule movements

Infected megakaryocytes were transferred onto video chambers maintained at 37°C. Cells were viewed on a microscope (Axiovert 200) equipped with a 63× oil immersion objective, and images were obtained using a CCD camera (Hamamatsu Photonics). Videos 1–4 were prepared using MetaMorph. Pictures of preplatelets expressing GFP–β1-tubulin were captured at 30-, 45-, or 60-s intervals over a course of 4 min. Pictures of EB3-GFP–expressing proplatelets were acquired every 2–5 s with a mean image capture time of 500 ms. The velocity of EB3-GFP comets was determined by dividing the distances traveled by the time elapsed. We included only comets that could be followed for a minimum of 15 s. To visualize α-granules, isolated megakaryocytes (day 4 in culture) were incubated overnight with 150 µg/ml Oregon green 488 human fibrinogen conjugate (Invitrogen) and 100 U/ml Hirudin from leeches (Sigma-Aldrich) in DME (Harrison et al., 1989). Megakaryocytes were then washed by albumin gradient sedimentation, and the resuspended pellet was placed in a video chamber. Images were acquired at 1-min intervals over a course of 36 min.

Released proplatelets cultured under continuous shear

Released proplatelets isolated from fetal liver–derived megakaryocytes were cultured at 37°C for up to 2 h in an incubator shaker (C24KC; New Brunswick Scientific) at 150 rpm, and shear forces were estimated to reach ~0.5 Pa maximally. Sample aliquots were collected every 20 min, and proplatelet counts were determined by flow cytometric analysis. Samples were then fixed, centrifuged, and probed with a rabbit polyclonal antibody against the C-terminal sequence of mouse β1-tubulin (LEDSEEDAEEAEVEAEDKDH; Genemed Synthesis, Inc.). Images were acquired using a confocal microscope (TCS SP5; Leica) equipped with a programmable xyz stage using a 20× 0.40 NA dry objective. Quantitative analysis was performed in MATLAB (The MathWorks, Inc.) and ImageJ (National Institutes of Health) using author-coded software. Objects were categorized based on area measurements and normalized to initial (time 0) object counts.

Preparation of photomicrographs

The digital images produced in MetaMorph were assembled into composite images using ImageJ and Photoshop (CS3; Adobe). Dividing lines explicitly separate different images or separate regions of the same image. No specific features within an image were enhanced, obscured, moved, removed, or introduced, and adjustments made to the brightness, contrast, and color balance were linearly applied to the whole image.

Online supplemental material

Fig. S1 illustrates the isolation of specific stages of megakaryocyte development and platelet production. Fig. S2 shows the quantification of platelet release during cell culture. Fig. S3 shows EB3-GFP movements in a released barbell proplatelet. Fig. S4 demonstrates the quantitation of cultured proplatelets by immunofluorescence microscopy. Fig. S5 shows multivesicular bodies present in human proplatelets. Video 1 shows microtubule dynamics during the conversion preplatelets into barbell proplatelets. Video 2 shows α-granule sorting during preplatelet to proplatelet interconversion. Video 3 shows α-granules sorting between the platelet-sized ends of a barbell proplatelet. Video 4 shows EB3-GFP movements in a released barbell proplatelet. Online supplemental material is available at http://www.jcb.org/cgi/content/full/jcb.201006102/DC1.

A. Ehrlicher gratefully acknowledges support from Thomas Stossel.

This work was supported in part by the National Institutes of Health (grant HL68130 to J.E. Italiano and training grant HL007680 to A. Ehrlicher), the National Institute of Dental and Craniofacial Research (short-term research training grant DE07268 to A. Montalvo), and the American Society of Hematology (2005 Trainee Award to A. Montalvo). We gratefully acknowledge D.A. Weitz and the Harvard Materials Research and Engineering Center (DMR-0213805) for confocal imaging. J.E. Italiano is an American Society of Hematology Junior Faculty Scholar.

Submitted: 16 June 2010
Accepted: 18 October 2010

References

Baker, G.R., P.M. Sullam, and J. Levin. 1997. A simple, fluorescent method to internally label platelets suitable for physiological measurements. *Am. J. Hematol.* 56:17–25. doi:10.1002/(SICI)1096-8652(199709)56:1<17::AID-AJH4>3.0.CO;2-5

Becker, R.P., and P.P. De Bruyn. 1976. The transmural passage of blood cells into myeloid sinusoids and the entry of platelets into the sinusoidal circulation; a scanning electron microscopic investigation. *Am. J. Anat.* 145:183–205. doi:10.1002/aja.1001450204

Behnke, O. 1969. An electron microscope study of the rat megacaryocyte. II. Some aspects of platelet release and microtubules. *J. Ultrastruct. Res.* 26:111–129. doi:10.1016/S0022-5320(69)90039-2

Behnke, O., and A. Forer. 1998. From megakaryocytes to platelets: platelet morphogenesis takes place in the bloodstream. *Eur. J. Haematol. Suppl.* 61:3–23.

Choi, E.S., J.L. Nichol, M.M. Hokom, A.C. Hornkohl, and P. Hunt. 1995. Platelets generated in vitro from proplatelet-displaying human megakaryocytes are functional. *Blood.* 85:402–413.

Drachman, J.G., D.F. Sabath, N.E. Fox, and K. Kaushansky. 1997. Thrombopoietin signal transduction in purified murine megakaryocytes. *Blood.* 89:483–492.

Handagama, P.J., B.F. Feldman, N.C. Jain, T.B. Farver, and C.S. Kono. 1987. Circulating proplatelets: isolation and quantitation in healthy rats and in rats with induced acute blood loss. *Am. J. Vet. Res.* 48:962–965.

Harrison, P., B. Wilbourn, N. Debili, W. Vainchenker, J. Breton-Gorius, A.S. Lawrie, J.M. Masse, G.F. Savidge, and E.M. Cramer. 1989. Uptake of plasma fibrinogen into the alpha granules of human megakaryocytes and platelets. *J. Clin. Invest.* 84:1320–1324. doi:10.1172/JCI114300

Heijnen, H.F., N. Debili, W. Vainchencker, J. Breton-Gorius, H.J. Geuze, and J.J. Sixma. 1998. Multivesicular bodies are an intermediate stage in the formation of platelet alpha-granules. *Blood.* 91:2313–2325.

Hoffmeister, K.M., T.W. Felbinger, H. Falet, C.V. Denis, W. Bergmeier, T.N. Mayadas, U.H. von Andrian, D.D. Wagner, T.P. Stossel, and J.H. Hartwig. 2003a. The clearance mechanism of chilled blood platelets. *Cell.* 112:87–97. doi:10.1016/S0092-8674(02)01253-9

Hoffmeister, K.M., E.C. Josefsson, N.A. Isaac, H. Clausen, J.H. Hartwig, and T.P. Stossel. 2003b. Glycosylation restores survival of chilled blood platelets. *Science.* 301:1531–1534. doi:10.1126/science.1085322

Italiano, J.E. Jr., and E.M. Battinelli. 2009. Selective sorting of alpha-granule proteins. *J. Thromb. Haemost.* 7:173–176. doi:10.1111/j.1538-7836.2009.03387.x

Italiano, J.E. Jr., P. Lecine, R.A. Shivdasani, and J.H. Hartwig. 1999. Blood platelets are assembled principally at the ends of proplatelet processes produced by differentiated megakaryocytes. *J. Cell Biol.* 147:1299–1312. doi:10.1083/jcb.147.6.1299

Italiano, J.E. Jr., W. Bergmeier, S. Tiwari, H. Falet, J.H. Hartwig, K.M. Hoffmeister, P. André, D.D. Wagner, and R.A. Shivdasani. 2003. Mechanisms and implications of platelet discoid shape. *Blood.* 101:4789–4796. doi:10.1182/blood-2002-11-3491

Italiano, J.E. Jr., S. Patel-Hett, and J.H. Hartwig. 2007. Mechanics of proplatelet elaboration. *J. Thromb. Haemost.* 5:18–23. doi:10.1111/j.1538-7836.2007.02487.x

Josefsson, E.C., H.H. Gebhard, T.P. Stossel, J.H. Hartwig, and K.M. Hoffmeister. 2005. The macrophage alphaMbeta2 integrin alphaM lectin domain mediates the phagocytosis of chilled platelets. *J. Biol. Chem.* 280:18025–18032. doi:10.1074/jbc.M501178200

Junt, T., H. Schulze, Z. Chen, S. Massberg, T. Goerge, A. Krueger, D.D. Wagner, T. Graf, J.E. Italiano Jr., R.A. Shivdasani, and U.H. von Andrian. 2007. Dynamic visualization of thrombopoiesis within bone marrow. *Science.* 317:1767–1770. doi:10.1126/science.1146304

Kessel, R.G., and R.H. Kardon. 1979. Circulating blood, blood vessels, and bone marrow. *In* Tissues and organs: a text-atlas of scanning electron microscopy. W.H. Freeman and Company, San Francisco. 35–50.

Lecine, P., J.L. Villeval, P. Vyas, B. Swencki, Y. Xu, and R.A. Shivdasani. 1998. Mice lacking transcription factor NF-E2 provide in vivo validation of the proplatelet model of thrombocytopoiesis and show a platelet production defect that is intrinsic to megakaryocytes. *Blood.* 92:1608–1616.

Lecine, P., J.E. Italiano Jr., S.W. Kim, J.L. Villeval, and R.A. Shivdasani. 2000. Hematopoietic-specific beta 1 tubulin participates in a pathway of platelet biogenesis dependent on the transcription factor NF-E2. *Blood.* 96:1366–1373.

Leven, R.M. 1987. Megakaryocyte motility and platelet formation. *Scanning Microsc.* 1:1701–1709.

Leven, R.M., and M.K. Yee. 1987. Megakaryocyte morphogenesis stimulated in vitro by whole and partially fractionated thrombocytopenic plasma: a model system for the study of platelet formation. *Blood.* 69:1046–1052.

Patel-Hett, S., J.L. Richardson, H. Schulze, K. Drabek, N.A. Isaac, K. Hoffmeister, R.A. Shivdasani, J.C. Bulinski, N. Galjart, J.H. Hartwig, and J.E. Italiano Jr. 2008. Visualization of microtubule growth in living platelets reveals a dynamic marginal band with multiple microtubules. *Blood.* 111:4605–4616. doi:10.1182/blood-2007-10-118844

Radley, J.M., and G. Scurfield. 1980. The mechanism of platelet release. *Blood.* 56:996–999.

Richardson, J.L., R.A. Shivdasani, C. Boers, J.H. Hartwig, and J.E. Italiano Jr. 2005. Mechanisms of organelle transport and capture along proplatelets during platelet production. *Blood.* 106:4066–4075. doi:10.1182/blood-2005-06-2206

Schulze, H., M. Korpal, W. Bergmeier, J.E. Italiano Jr., S.M. Wahl, and R.A. Shivdasani. 2004. Interactions between the megakaryocyte/platelet-specific beta1 tubulin and the secretory leukocyte protease inhibitor SLPI suggest a role for regulated proteolysis in platelet functions. *Blood.* 104:3949–3957. doi:10.1182/blood-2004-03-1179

Schwertz, H., S. Köster, W.H. Kahr, N. Michetti, B.F. Kraemer, D.A. Weitz, R.C. Blaylock, L.W. Kraiss, A. Greinacher, G.A. Zimmerman, and A.S. Weyrich. 2010. Anucleate platelets generate progeny. *Blood.* 115:3801–3809. doi:10.1182/blood-2009-08-239558

Shivdasani, R.A. 2001. Molecular and transcriptional regulation of megakaryocyte differentiation. *Stem Cells.* 19:397–407. doi:10.1634/stemcells.19-5-397

Shivdasani, R.A., and S.H. Orkin. 1996. The transcriptional control of hematopoiesis. *Blood.* 87:4025–4039.

Shivdasani, R.A., M.F. Rosenblatt, D. Zucker-Franklin, C.W. Jackson, P. Hunt, C.J. Saris, and S.H. Orkin. 1995. Transcription factor NF-E2 is required for platelet formation independent of the actions of thrombopoietin/MGDF in megakaryocyte development. *Cell.* 81:695–704. doi:10.1016/0092-8674(95)90531-6

Sullivan, M.T., R. Cotten, E.J. Read, and E.L. Wallace. 2007. Blood collection and transfusion in the United States in 2001. *Transfusion.* 47:385–394. doi:10.1111/j.1537-2995.2007.01128.x

Tablin, F., M. Castro, and R.M. Leven. 1990. Blood platelet formation in vitro. The role of the cytoskeleton in megakaryocyte fragmentation. *J. Cell Sci.* 97:59–70.

Tavassoli, M., and M. Aoki. 1981. Migration of entire megakaryocytes through the marrow—blood barrier. *Br. J. Haematol.* 48:25–29. doi:10.1111/j.1365-2141.1981.00025.x

van Nispen tot Pannerden, H., F. de Haas, W. Geerts, G. Posthuma, S. van Dijk, and H.F. Heijnen. 2010. The platelet interior revisited: electron tomography reveals tubular alpha-granule subtypes. *Blood.* 116:1147–1156. doi:10.1182/blood-2010-02-268680

Youssefian, T., and E.M. Cramer. 2000. Megakaryocyte dense granule components are sorted in multivesicular bodies. *Blood.* 95:4004–4007.